International Journal of Physical Sciences Vol. 7(46), pp. 6093-6104, 9 December, 2012
Available online at http://www.academicjournals.org/IJPS
DOI: 10.5897/IJPS12.406
ISSN 1992-1950 ©2012 Academic Journals

*Full Length Research Paper*

# Wind energy conversion system with full-scale power converter and squirrel cage induction generator

**Bouaziz Béchir[1], Bacha Faouzi[1]* and Moncef Gasmi[2]**

[1]University of Tunis, ESSTT, 5 Av Taha Hussein, B. P. 56, Montfleury 1008, Tunis, Tunisie.
[2]National Institute of Applied Sciences and Technology (INSAT) Centre Urbain Nord, B. P. 676, 1080 Tunis Cedex, Tunisie.

Accepted 20 June, 2012

**This paper describes a modeling and control of a variable speed squirrel-cage induction generator with back to back power electronics converters used in variable speed wind energy conversion system. The power electronics is composed of the generator side converter (GSC) coupling to the grid connected converter (GCC) together via DC bus capacitor. The generator side converter (GSC) is controlled by direct torque control (DTC). The control objectives of the generator side converter (GSC) are to optimize the energy capture from the wind turbine and supply the magnetic flux to the squirrel cage induction generator (SCIG). The GCC converter delivering the energy from the machine side to the utility grid regulated the DC link voltage and the power flows to the grid. The basic idea of P-Q control method used is based on voltage vector oriented control and decoupling in the d-q axis reference frame. The complete control system has been developed; analyzed and validated by Matlab simulation. The two operating modes of GCC converter and the performance under active and reactive power variations are also presented. The low voltage ride-through (LVRT) performances of the variable speed wind turbine (VSWT) is tested, when the grid voltage has dropped to a very low value. Simulation results confirmed the effectiveness of the proposed control strategies and their capability under different case study.**

**Key words:** Variable speed wind turbine, converter control, power quality, back to back converters, vector oriented control.

## INTRODUCTION

Global warming is accelerating due to the effects of climate change, and investments are increasing in new alternative power sources to replace existing fossil fuels. Among the new and renewable energy sources, wind energy is the clean energy and it rapid growth for the electricity production (Haejoon et al., 2012). There are different configurations of wind turbine system. The use of squirrel-cage induction generators (SCIG) for direct grid-connection wind energy conversion systems (WECS) is well established. With the last advances in power electronics, the use of variable-speed SCIG with a double stage AC/DC/AC power conversion has become quite attractive (Watthan and Bunlung, 2011; Shahab et al., 2011), in both low power and very high power levels, increased energy production at low wind and elimination of the excitation capacitor bank.

The variable speed wind turbine is replacing constant speed wind turbine (CSWT) types to control rotation speed and improve efficiency with respect to the wind velocity. The wind velocity is not constant, and there is a rotation speed for a given wind velocity for which the WT output is maximum (Whei et al., 2010). Thus, it is necessary to operate the WT at variable speeds to change the rotation speed according to the wind velocity. The double-fed asynchronous generator and the permanent-magnetic synchronous generators, which are used for variable speed generation, are not directly connected to the grid; an electronic power converter is installed between the generator and the grid.

Recently, generators that use a SCIG for fixed speed generation have been upgraded to the variable speed generation type that can generate power for the entire section, as with PMSG, by adding a full-scale power converter with the same capacity as the generator

*Corresponding author. E-mail: Faouzi.Bacha@esstt.rnu.tn.

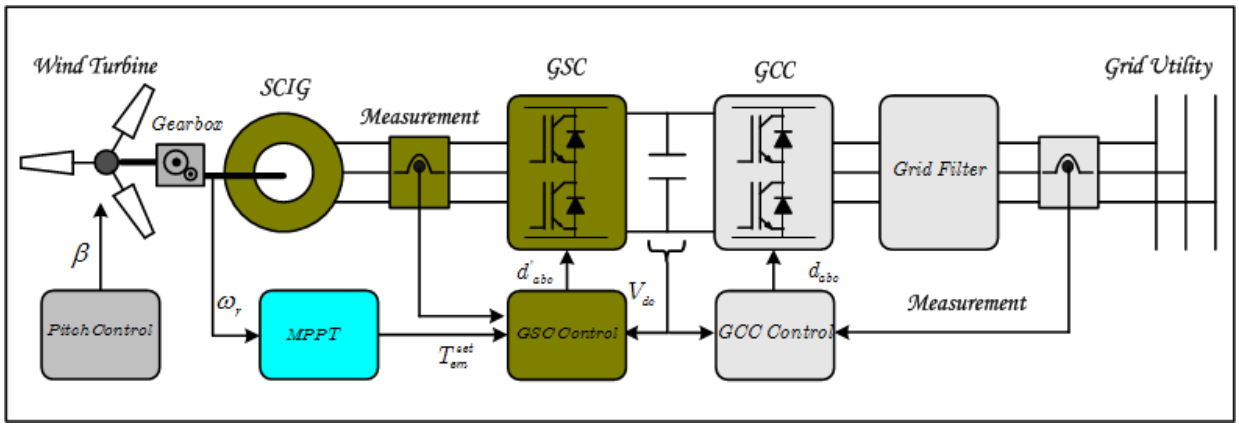


**Figure 1.** Variable speed squirrel-cage induction generator wind turbine.

(Bouaziz et al., 2012). A variable speed WT with SCIG can perform variable speed generation at lower cost compared to PMSG, and solve the problem of the narrow generation area used in existing fixed speed generation. Thus, variable speed WTs are economically important. In order to keep power quality under limits proposed by standards, it is necessary to include this in control objectives. There are several technical issues arising from the complexity of control operation.

This paper focuses on a control methodology for improving the deficiency of the CSWT. The deficiency can be improved by the back to back converter is composed of two voltage source converters connected together via a dc-bus capacitor. First converter stays between the SCIG and the DC bus capacitor called GSC. The function of the GSC is to produce the machine flux for the SCIG and to optimum the energy capture from the wind. The second converter stays between the DC bus capacitor and the grid called GCC. The function of this converter is to regulate the DC-bus voltage and active and reactive powers flows. It has two operating modes: rectifying mode and inverting mode. When the dc-bus voltage is reduced, the GCC operated in rectifying mode and to charge the capacitor to regulate the dc-bus voltage. When there is energy from the wind, the DC-bus voltage increases and the GCC operates in inverting mode to supply the energy from the DC bus to the utility grid and regulate the DC link voltage and the powers flows.

## MODEL OF SQUIRREL-CAGE INDUCTION GENERATOR WIND TURBINE

A detailed model of the wind turbine is illustrated in Figure 1. The components of the wind turbine include a three bladed rotor with corresponding pitch controller, a mechanical gearbox, a SCIG with a full-scale back-to-back converter, DC link capacitor and a line filter and converter controllers. The mechanical torque of the wind turbine is converted to electrical power at the stator of the SCIG. The variable speed operation of the wind turbine is possible by using a converter, which can be obtained by controlling the electromagnetic toque. The grid connected converter is connected to the external power network through a filter, and sets the maximum output power while maintaining the voltage of the DC link within the allowable range.

### Modeling of the wind turbine

The mechanical part of the wind turbine consists of a rotor blade, a pitch control and a gearbox. The mechanical power can be expressed as:

$$P_m = \frac{\rho}{2} A v^3 C_p(\lambda, \beta) \quad (1)$$

The output mechanical torque can be calculated from the following equations:

$$T_m = \frac{\rho}{2} A v^2 C_T(\lambda, \beta) \quad (2)$$

$$C_T(\lambda, \beta) = \frac{C_p(\lambda, \beta)}{\lambda} \quad (3)$$

In this paper, the first order model is used to describe the dynamic of the wind turbine and is written by

$$J \frac{d\omega_r}{dt} = T_m - T_e \quad (4)$$

The electrical torque at the optimum operating speed is given by:

$$T_e = T_e^{set} = K_{opt}\ \omega_r^2 \quad (5)$$

Substituting (5) into (4), then

$$J \frac{d\omega_r}{dt} = T_m - K_{opt} \omega_r^2 \quad (6)$$

Where, $C_p$ presents the wind turbine power conversion efficiency. It is a function of the tip speed ratio $\lambda$, as well as the blade pitch

**Table 1.** Parameters of the performance power coefficient.

| $c_1$ | $c_2$ | $c_3$ | $c_4$ | $c_5$ | $c_6$ | $c_7$ | $c_8$ |
|---|---|---|---|---|---|---|---|
| 0.5109 | 116 | 0.4 | 5 | 21 | 0.0068 | 0.08 | 0.035 |

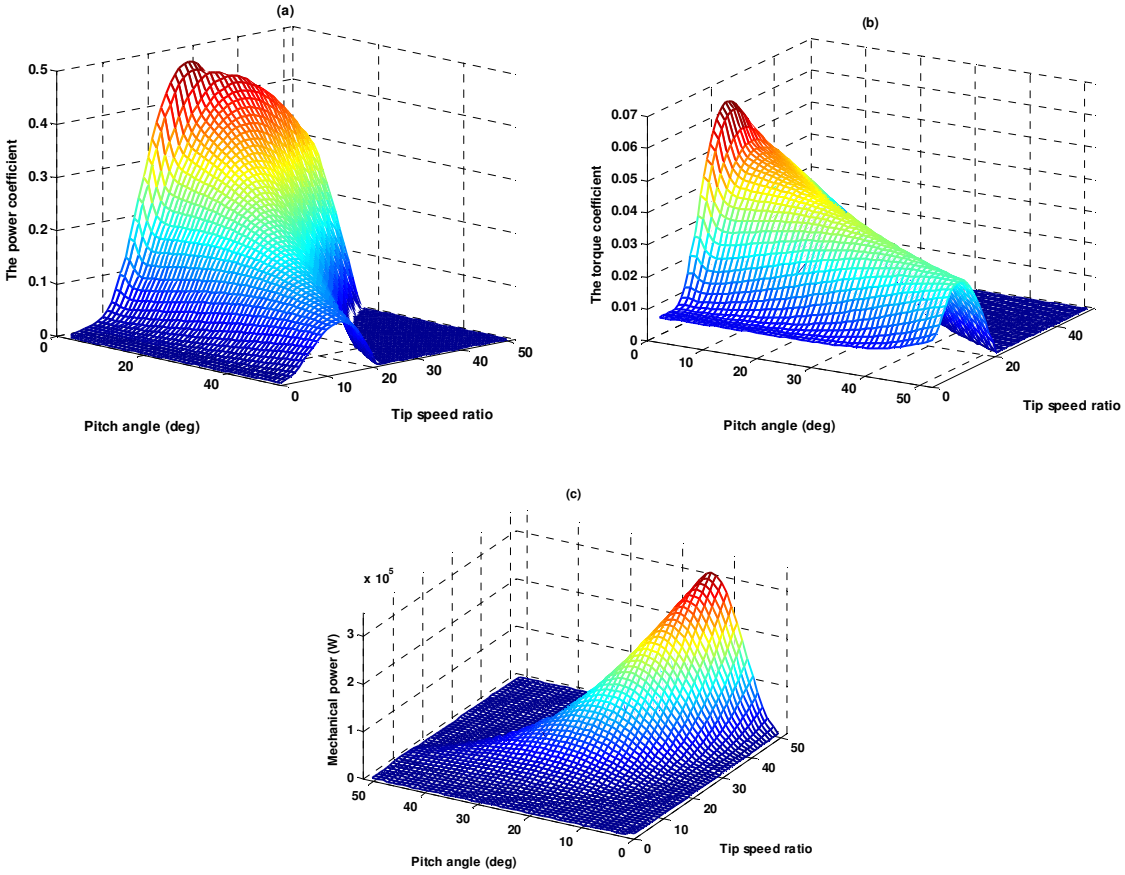


**Figure 2.** Characteristics of the wind turbine. (a) Power coefficient. (b) Torque coefficient. (c) Mechanical power.

angle $\beta$ in a pitch controlled wind turbine. The parameter $\lambda$ is defined as the ratio of the tip speed of the turbine blades to wind speed, and is given by:

$$\lambda = \frac{v_t}{v} = K_{gear}\ \frac{2R\omega_r}{\rho v} \tag{7}$$

The power coefficient is a function of tip speed ratio and blade pitch angle and can be approximated by substituting (3) into 8:

$$C_p(\lambda,\beta) = c_1\left(\frac{c_2}{X} - c_3\beta - c_4\right)\exp\left(-\frac{c_5}{X}\right) + c_2\lambda$$

Where

$$X = \frac{1}{\lambda + c_7\beta} - \frac{c_8}{\beta^3 + 1} \tag{8}$$

The coefficient $c_1$ - $c_8$ depends on the wind turbines. To obtain correct Cp curve for turbine used in this paper $c_1$ - $c_8$ are proposed as shown in Table 1.

The characteristics of the wind turbine, for different values of the pitch angle are illustrated in Figure 2. Figure 2 indicates that there is one specific tip speed ratio at which the turbine is most efficient. Normally, a variable speed wind turbine follows the optimal power coefficient to capture the maximum power up to the rated speed by varying the rotor speed to keep the system at optimal tip speed ratio. Then, it operates at the rated power with power control during high wind speed by active control of the blade pitch angle.

## Pitch control

The pitch angle controller with the wind turbine is used to limit the output power at the terminal of the induction generator when the wind speed is over the rated speed. When wind speed exceeds its nominal value, the speed of aerodynamic rotor and power produced

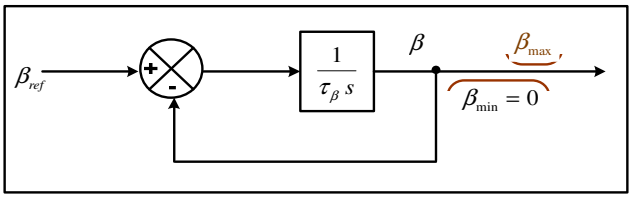


**Figure 3.** Pitch angle controller.

by the turbine increase. This is unwanted phenomenon, which is providing to damage of the wind turbine. The pitch control can be used to avoid this apparition. The speed of the rotor for stronger winds can be limited and kept constant at the rated value by changing the pitch angle of the blades. The principle of this method illustrated by Figure 3 is explained on wind turbine designed for nominal wind speed equal to 12 m/s.

### Squirrel-cage induction generator model (SCIG)

The electric part of the wind turbine largely consists of a SCIG and a full-scale back-to-back converter. The SCIG was represented by the following equations:

$$\begin{aligned}
\frac{di_\alpha}{dt} &= \frac{1}{\sigma}\left(\frac{1}{\tau_s}+\frac{1}{\tau_r}\right)i_\alpha - \omega i_\beta - \frac{1}{\tau_r l_s}\lambda_\alpha + \frac{\omega}{l_s}\lambda_\alpha + \frac{1}{l_s}v_\alpha \\
\frac{di_\beta}{dt} &= -\omega i_\alpha + \frac{1}{\sigma}\left(\frac{1}{\tau_s}+\frac{1}{\tau_r}\right)i_\beta - \frac{\omega}{l_s}\lambda_\alpha + \frac{1}{\tau_r l_s}\lambda_\beta + \frac{1}{l_s}v_\beta \\
\frac{d\lambda_\alpha}{dt} &= -R_s i_\alpha + v_\alpha \\
\frac{d\lambda_\beta}{dt} &= -R_s i_\alpha + v_\beta
\end{aligned} \tag{9}$$

With

$$l_s = \sigma L_s,\ \sigma = 1 - \frac{L_m^2}{L_s L_r},\ m_r = \frac{L_m}{L_r},\ \tau_r = \frac{L_r}{R_r},\ \tau_s = \frac{L_s}{R_s}$$

### Back-to- back converter model

The mathematical model of a back-to-back converter can be obtained from descriptions of the relationship between the supply, converter voltages and line currents in Concordia reference frame. The remaining electrical parts of the system are generator side converter (GSC) and the grid connected converter (GCC). The generator side converter (GSC) is identical in design to the GCC converter. The stator voltage components of the induction machine in Concordia referential frame are given by:

$$v_a = d'_a V_{dc} \tag{10}$$

$$v_b = d'_b V_{dc} \tag{11}$$

$$i_{dc} = \frac{3}{2}\left(i_b d'_a + i_a d'_b\right) \tag{12}$$

As a result, the full model of the grid, capacitor and GCC converter is summarized by the expressions below:

$$L\frac{di_{gk}}{dt} + Ri_{gk} = -u_{gk} + \left(V_{dc}d_j - \frac{V_{dc}}{3}\sum_{j=1}^{3} d_j\right) \tag{13}$$

$$C\frac{dV_{dc}}{dt} = i_{dc} - \sum_{k=j=1}^{3} d_j i_{gk} \tag{14}$$

### RL filter on the grid connected converter

The GCC converter is connected to the grid through a RL filter. According to the stationary reference frame can be expressed the electrical model:

$$\begin{aligned}
L_f\frac{di_{gd}}{dt} &= u_{gd} - R_f i_{gd} + \omega_g L_f i_{gq} \\
L_f\frac{di_{gq}}{dt} &= u_{gq} - R_f i_{gq} + \omega_g L_f i_{gd}
\end{aligned} \tag{15}$$

## BACK-to-BACK CONVERTER CONTROLLER DESIGN

The back to back converter control module consists of a generator-side converter controller, a grid connected converter controller, and a dc-link controller. Here, $P_g^{set}$ and $Q_g^{set}$ are the references of the active and reactive power injected to the grid.

The active power reference $P_g^{set}$ is determined by the closed-loop of the dc-link voltage. The reactive power reference $Q_g^{set}$ can be set following the requirements of the grid management service. It can satisfy the unity power factor (UPF) operation of the GCC converter by setting $Q_g^{set}$ to zero.

### Generator side converter controller

Figure 4 shows a block diagram of the generator-side converter controller module that consists of direct torque control (DTC). It is well known that the basic concept of DTC based drives is to control both stator flux and electromagnetic torque simultaneously. In the conventional DTC approach initiated by Takahashi, these reference values are ensured by direct selection of a suitable voltage vector. In Figure 4, the generator electromagnetic torque reference is obtained by the MPPT control method proposed.

### The MPPT tracking

The power of the turbine is optimized by an MPPT algorithm. The control consists of varying the speed of the turbine in order to remain the ratio of the tip speed at around its optimum value. The power coefficient of the turbine is equal to its maximum value. In these conditions the maximum power is given by:

$$P_{\max} = K_{opt}\omega_r^3 \tag{16}$$

With $K_{opt} = 0.5\rho C_{p\max}\left(\frac{2R}{pK_{gear}\lambda_{opt}}\right)^3$

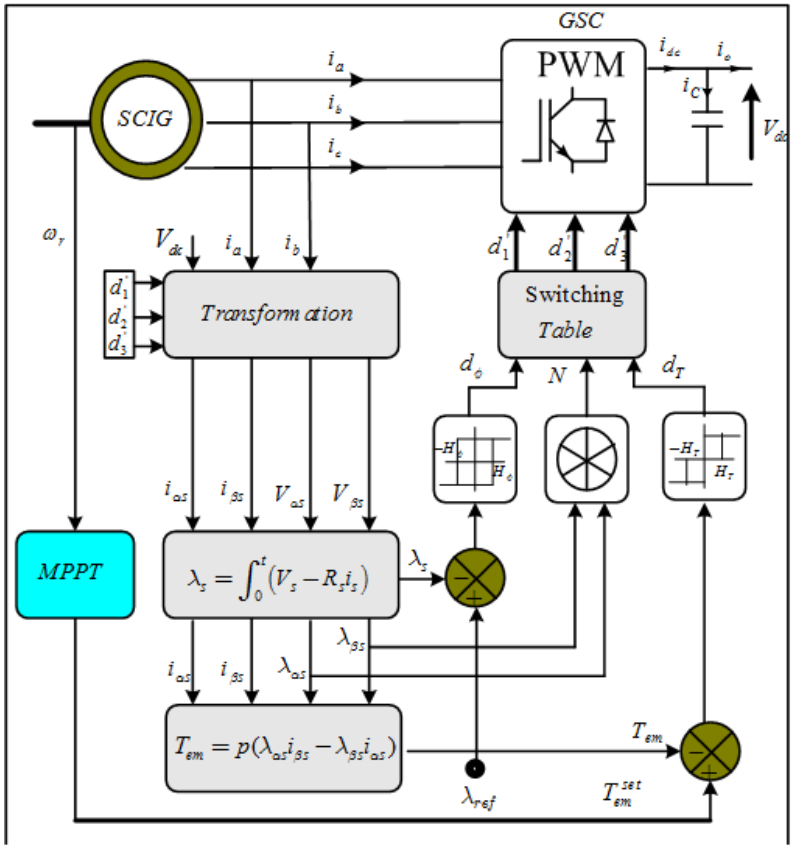


**Figure 4.** Schematic diagram of the DTC of generator side converter.

**Grid connected converter controller**

Figure 5 illustrates the proposed grid connected converter controller module consisting of vector oriented control (VOC). The aim of the GCC converter is to regulate the dc-link voltage and maintain the balance between the dc-link power and powers supplied to the grid. This is done by controlling the current axis component of the line side.

The active and reactive power given by:

$$P_g = \frac{3}{2}\left(u_{gd}\, i_{gd} + u_{gq}\, i_{gq}\right)$$
$$Q_g = \frac{3}{2}\left(u_{gq}\, i_{gd} - u_{gd}\, i_{gq}\right) \quad (17)$$

The basic principle of the vector oriented control method is to control the instantaneous active and reactive grid currents and, consequently, the active and reactive power, by separate controllers. The grid voltages and currents are first sensed. By means of the phase locked loop (PLL), the grid angle and frequency can be detected in order to synchronize the voltage output of the grid connected converter with grid. The demanded amount of power is first estimated from the utility grid at the desired power factor, in consequence, the sets values of currents in a synchronous reference frame synchronized with grid voltage are calculated. Consequently, the current controllers are trying to bring the actual currents to its references. So far is how the controller could be constructed. When we impose set values of active and reactive powers, we can determine the current references:

$$i_{gd}^{set} = \frac{2}{3}\frac{\left(u_{gd} P_g^{set} + u_{gq} Q_g^{set}\right)}{\left(u_{gd}^2 + u_{gq}^2\right)}$$
$$i_{gq}^{set} = \frac{2}{3}\frac{\left(u_{gq} P_g^{set} - u_{gd} Q_g^{set}\right)}{\left(u_{gd}^2 + u_{gq}^2\right)} \quad (18)$$

With the assumption of zero reactive power command, the current command equations can be simplified such that:

$$i_{gd}^{set} = \frac{2}{3}\frac{P_g^{set}}{u_{gd}}$$
$$i_{gq}^{set} = 0 \quad (19)$$

This paper employs the method of voltage decoupling control. Since we have the voltage cross coupling terms between the d-q axis is compensated by

$$u_{gd} = v_{gd} - \omega_g L_g i_{gd}$$
$$u_{gq} = v_{gq} + \omega_g L_g i_{gq} \quad (20)$$

Substituting (20) in (15), then

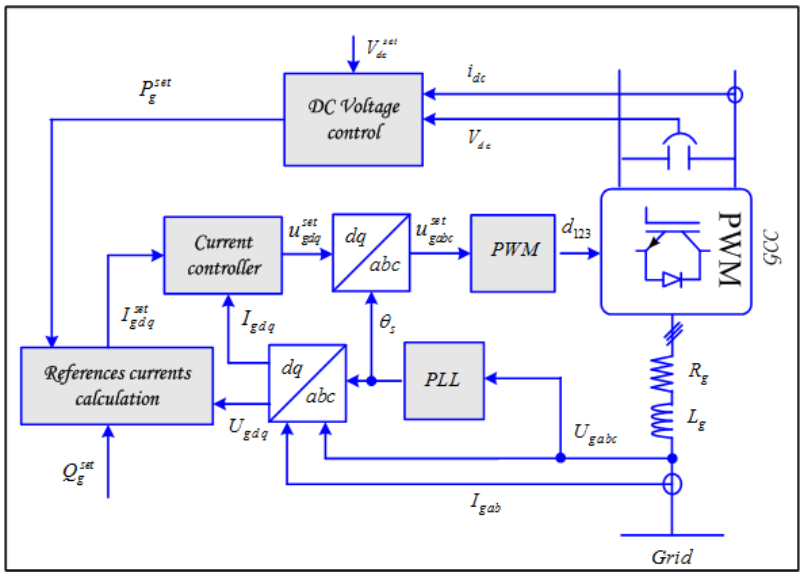


**Figure 5.** Control box diagram's of the proposed VOC GCC converter.

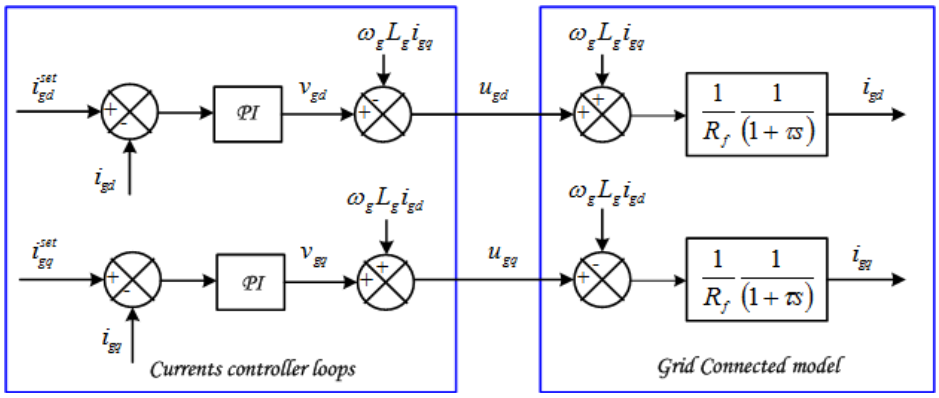


**Figure 6.** Decoupling between the d and q axes.

$$L_f \frac{di_{gd}}{dt} = v_{gd} - R_f i_{gd}$$
$$L_f \frac{di_{gq}}{dt} = v_{gq} - R_f i_{gq} \quad (21)$$

The voltage terminals are independent from the cross coupling term. They can be controlled separately for d-q axis. The grid connected converter and the regulation current loops can be described by the diagram bloc of Figure 6.

#### DC-link model and proposed controller

The capacitor in the dc-link voltage is an energy storage device. In describing the transit of the output power of the GSC to the grid. Figure 7 shows the dc-link model with its controller.
The power stocked in the capacitor

$$P_C = V_{dc} I_c^{set} \quad (22)$$

The power of the DC side is given by:

$$P_{dc} = V_{dc} I_{dc} \quad (23)$$

The set-value of the active power is determined by:

$$P_g^{set} = P_{dc} - P_C \quad (24)$$

## RESULTS AND DISCUSSION

### Operating mode of the GCC

In Figure 8 present the simulation results of the bidirectional PWM converter with a proposed vector oriented control (VOC) strategy and decoupling control of d-q current component. It has two operating modes:

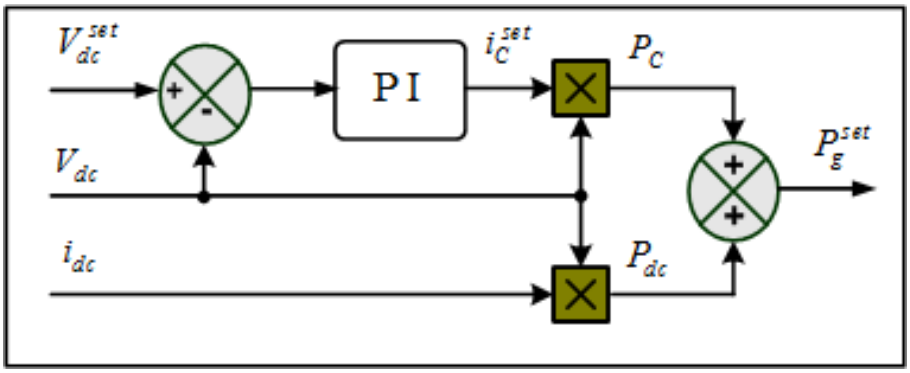


**Figure 7.** DC-link voltage modeling and proposed controller.

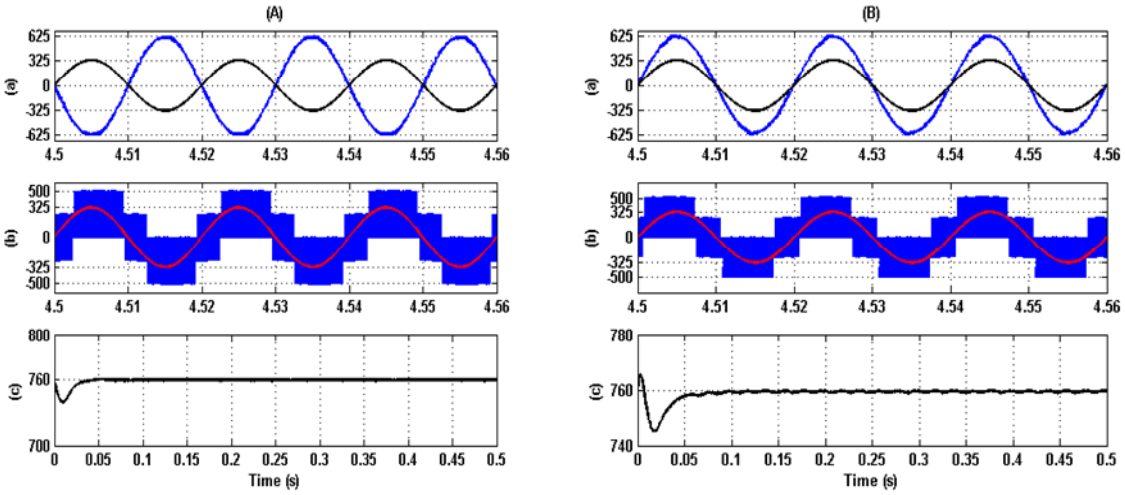


**Figure 8.** Simulation results using VOC control during operating mode of GCC converter. (a) AC current and voltage. (b) AC voltage and GCC converter voltage. (c) DC-bus voltage.

rectifying mode and inverting mode. It can be seen from Figure 8, that the proposed control strategy of direct power control ensures smooth control of active and reactive power and regulation of dc-bus voltage. The inversion of the power and confirm the desired power transfer. The response of the ac line current and ac voltage corresponding of two operating modes is presented in Figures 8 and shows the desired power flows between the DC-side to AC-side. Notice that, the DC- bus voltage follows its reference with a very low ripple.

### Power steps performance in GCC

Figure 9 shows the system response during various active and reactive power steps for the proposed control strategy of the GCC converter. The active power is stepped from 0 to 300 kW and exported from the converter to grid at 2.5 s and then backed to 0 at 2.54 s, while the reactive power is stepped from −100 kVar (inductive) to 100 kVar (capacitive) at 2.5 s and backed to −100 kVar at 2.54s. The transient response of both active and reactive powers for the proposed control scheme is within a few milliseconds, whereas the dynamic response of the proposed VOC control is largely dependent on the PI parameters of currents controller loops. Figure 9 shows also clearly that the control strategy has achieved much improved performance with well-smoothed active/reactive powers and ac currents.

### Turbulent wind speed

This section evaluates the overall operation of the variable speed squirrel cage induction generator by simulation results. The set of the proposed control strategies from Figure 10 illustrates the evolution of the

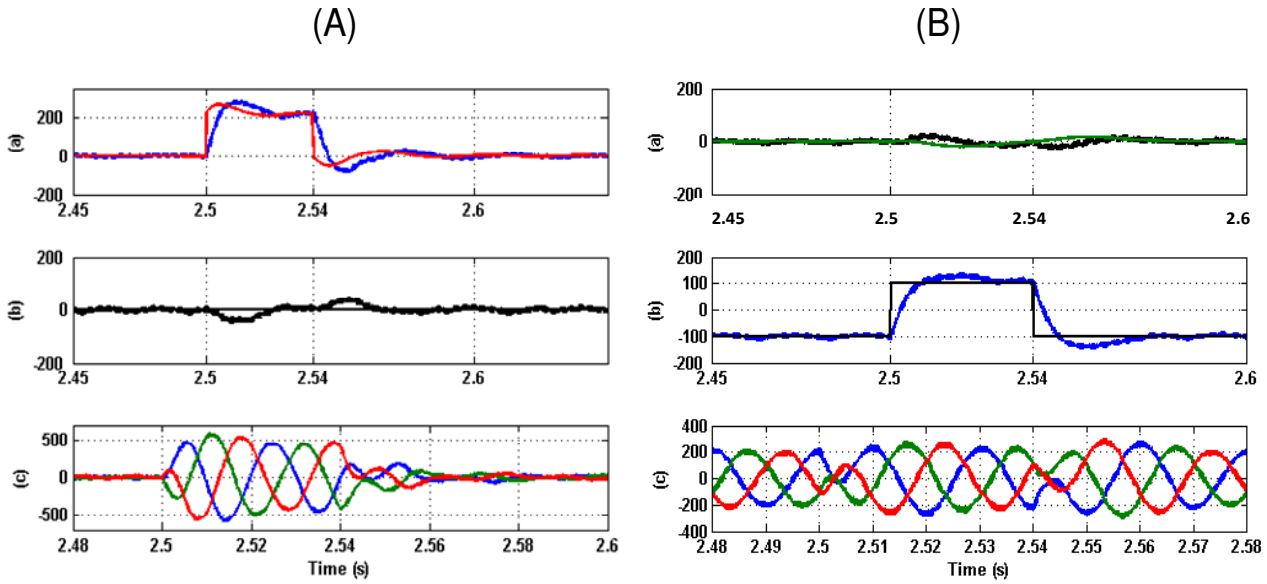


**Figure 9.** System responses during various active and reactive power steps (A) Inverting mode (B) Rectifying mode; (a) active power (kW). (b) reactive power (kVar). (c) three-phase AC currents.

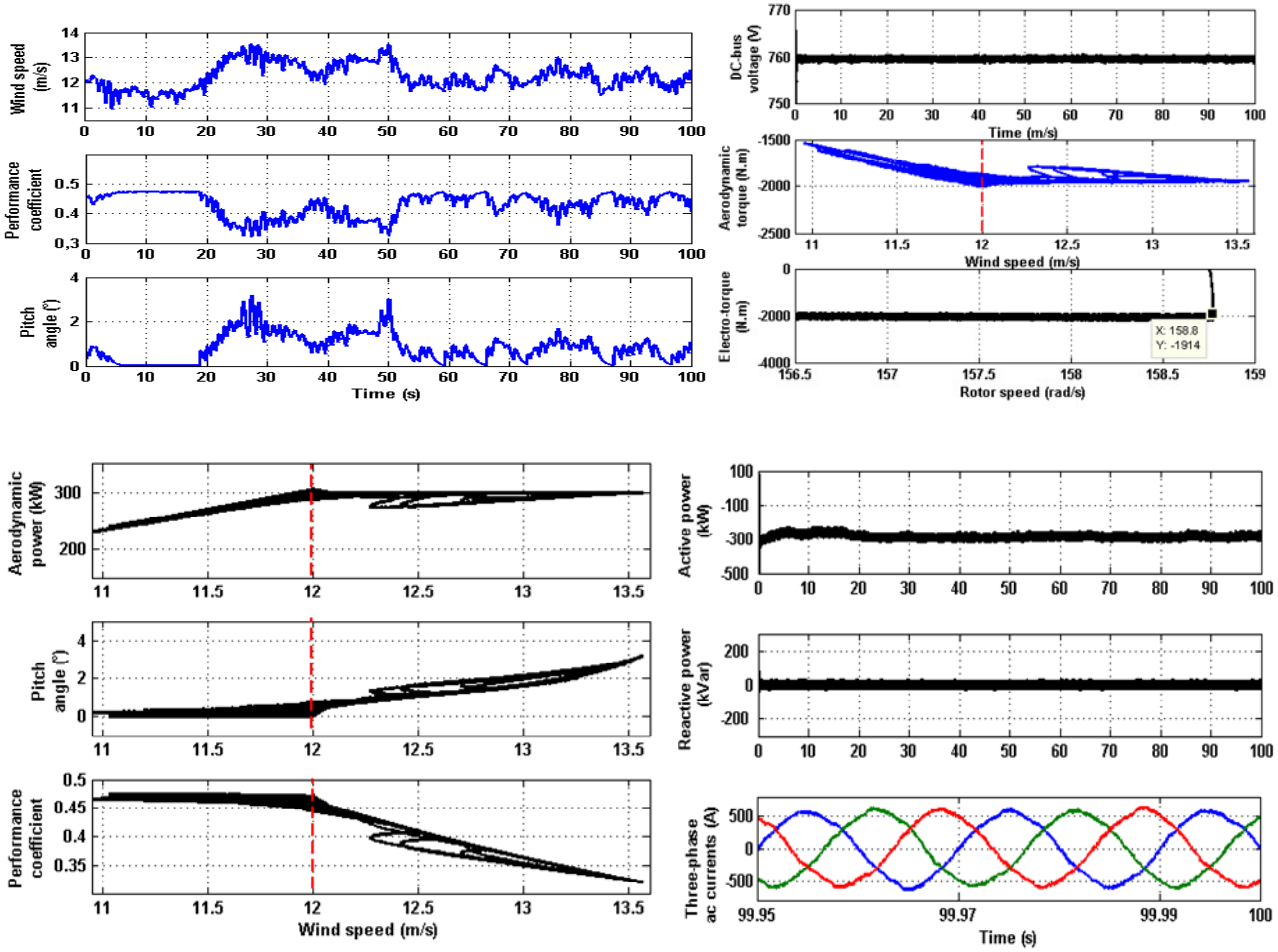


**Figure 10.** Simulation behavior of the Variable speed squirrel-cage induction generator wind turbine in a turbulent wind speed.

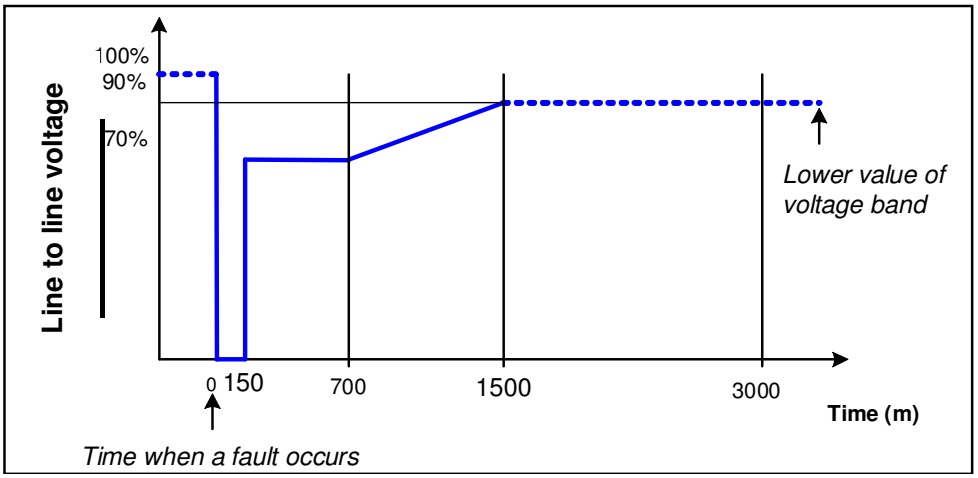


**Figure 11.** Voltage profile according to the requirements for LVRT capability of synchronous generators (Daunghom et al., 2010).

main electrical and mechanical variables under turbulent wind speed. Wind profile is presented in Figure 10. It can be observed that the wind is oscillating around the mean wind speed. The closed-loop VSWT manages to change its rotational speed, in order to optimum the energy capture from the wind turbine, according to imposed energy reliability. This control objective is accomplished, as it can be seen on the temporal evolution of the power coefficient and of the pitch control. The same conclusion can be drawn from the evolution of the aerodynamic power, pitch angle and from the power coefficient variation versus the wind speed. The pitch control objective has been accomplished. When the wind speed is over the rated speed, the aerodynamic power is limited on the set value. The control strategies objectives have been achieved, as it can be seen on the temporal evolution of the three phase ac currents, the DC-link voltage and the powers flow to the grid. Notice that, the DC bus voltage is maintained around its reference and the sinusoidal waveform of current injected to the grid is established.

The electrical and mechanical variables while a turbulent wind speed of 12 m/s will be influenced by the disturbance and therefore oscillating around their nominal value. The oscillations are transient and not considerable.

## Low voltage ride-through performances of the VSWT

In this section, the performance of the generator when affected by large faults or small disturbances is analyzed. Especially, the following effects are investigated. The grid code of most countries requires wind generators to stay connected in the case of grid faults (Low voltage ride-through capability (LVRT) or fault ride through capability (FRT)) (Daunghom et al., 2010). It is of particular importance to transmission system operators, that wind farms stay connected in case of faults at major transmission levels leading to a voltage depression in a wide area, which could lead to a major loss of wind generation if wind farms were not equipped with LVRT-capability. Therefore, LVRT-capability is a definite requirement for all larger wind farms (Daunghom et al., 2010).

The main issue of variable speed squirrel-cage induction generator wind turbine is their ability to remain in synchronism during and after major voltage sags. The following fault scenarios at the system are simulated. Three phase short-circuit with 150 ms clearing time (40% retain voltage), three phase short-circuit with 150 ms clearing time, (60% retain voltage) and three phase short-circuit with 150 ms clearing time, (80% retain voltage). The fault duration was chosen to be 150 ms, which represents a worst case assumption in the PEA system for first-zone fault clearing times. Additionally a voltage profile (Figure 11), according to the grid connection conditions from E.ON (Daunghom et al., 2010) for squirrel cage induction generator machines, is applied to the system and the generator response in this study is given.

Simulation results of a three-phase fault with 150 ms duration (80% retain voltage) at nominal wind speed conditions show according to Figure 12.

Simulation results of a three-phase fault with 150 ms duration (40 and 60% retain voltage) at nominal wind speed conditions show according to Figure 13.

Therefore, variable speed squirrel-cage induction generator wind turbine provides reactive power support in case of grid disturbances and to stay connected to the grid. In addition, the injected reactive current is enough to accomplish restrictive grid code requirements similar to the German operator E.ON Netz.

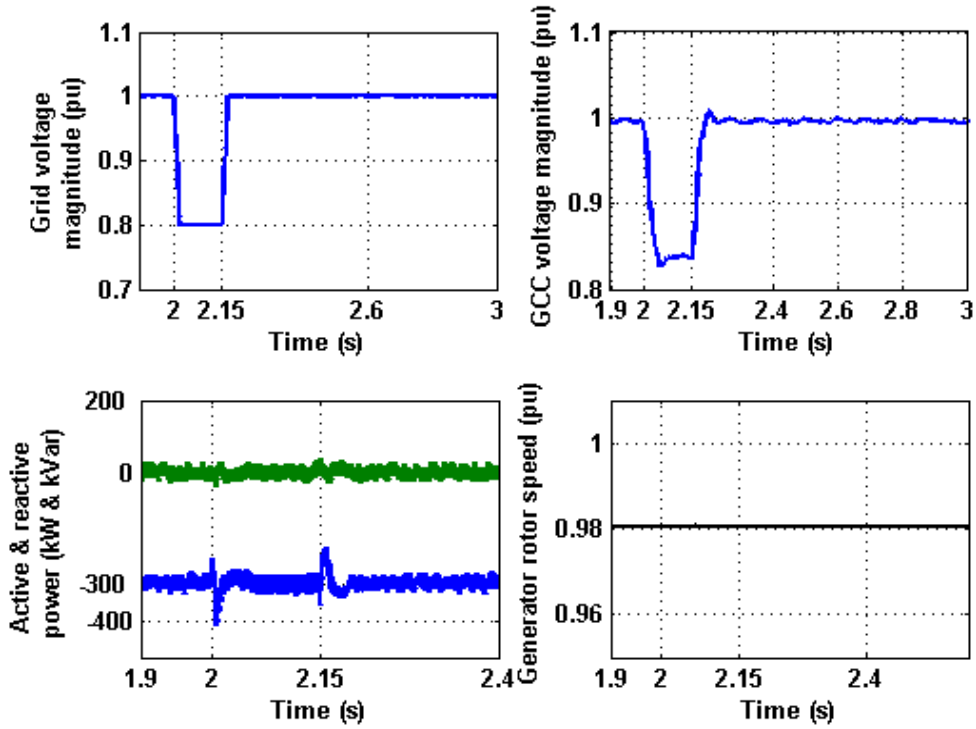


**Figure 12.** Simulation results of a three-phase fault with 150 ms duration (80% retain voltage).

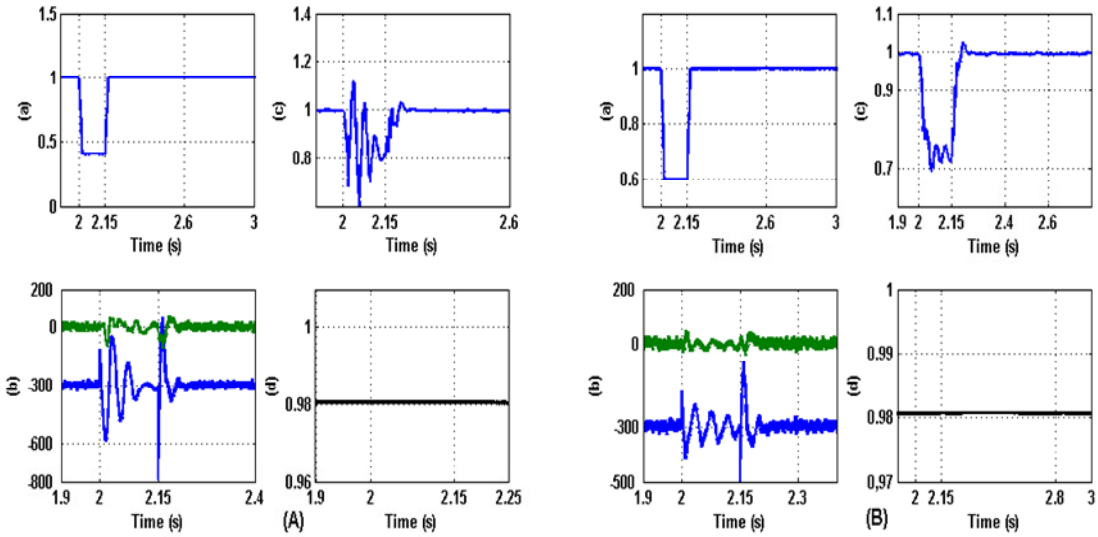


**Figure 13.** Simulation results of a three-phase fault with 150 ms duration. (A) 40% retain voltage, (B) 60% retain voltage; (a) Grid voltage magnitude (pu). (b) GCC converter voltage magnitude (pu). (c) Active and reactive power flows to the grid (Kw and kVar). (d) Generator rotor speed (pu).

## Conclusion

A control system for a variable speed squirrel cage induction generator driven by the wind turbine has been presented. A comprehensive control strategy for the wind generation system is suggested and developed. Generator side converter is controlled by direct torque control method and the grid connected converter is controlled by the vector oriented control method and decoupling control in the d-q axis reference frame. The

power extraction processes from the wind to the utility grid are cooperative between both converters. The generator side is operated forget the electrical energy from the wind to the DC bus capacitor and the grid connected is operated to transfer the power from the capacitor to the utility grid. The two operating modes and the decoupling control mode of the GCC converter give the capability of independent control of active and reactive powers with bidirectional power fellows. Compared to the technologies of variable speed wind turbines, variable speed squirrel-cage induction generator wind turbine has a number of substantial advantages due to its their ability to remain in synchronism during and after major voltage sags and the capability to keep power quality under limits proposed by standards (Appendix; Tables 1, 2 and 3).

**Nomenclature:** $C_p$, Power coefficient; $P_m$, The mechanical power; $T_m$, The mechanical torque; $T_e$, The electrical torque; $v$, Wind speed; $v_t$, Blade tip speed; $l$, Tip speed ratio; $b$, Pitch angle; $K_{gear}$, Gearbox ratio; $A$, Area swept by rotor blades; $w_r$, The rotational speed of the rotor, $u_{gd}, u_{gq}$, d-q axis voltage of grid connected converter; $i_{gd}, i_{gq}$, d-q axis current of grid connected converter; $l_a, l_b$, d-q axis flux of induction machine; $V_{dc}$, Dc bus voltage.

**REFERENCES**


Bouaziz B, Bacha F, Gasmi M (2012). A Fuzzy Direct Power Control for a Variable Speed Wind Turbine. Int. Rev. Aut. Cont (IREACO). 5(1).

Chong HNg, Ran L, Jim B (2008). Unbalanced grid fault ride through control for a wind turbine inverter. IEEE Trans. Ind. Appl. 44(3):845-856.

Daunghom K, Premrudeepreechacharn S (2011). Fault Ride-Through of Fully Enclosed Squirrel-Cage Induction Generators for Wind Farms in Thailand. Proc. IEEE Int. Conf. Trans. Distr. Expos. pp. 1-6.

Gandomkar A, Mahmoudi A, Pirasteh H, Parastar A, Kahourzade S (2011). Improvement of direct torque control in high power induction motors. Int. J. Phys. Sci. 6(12):2789-2798.

Giuseppe S, Jan S, Ambra S (2002). Improving Voltage Disturbance Rejection for Variable-Speed Wind Turbines. IEEE Trans. Energy Conv. 17(3):422-428.

Haejoon A, Heesang K, Hongwoo K, Hyungoo K, Seokwoo K, Gilsoo J, Byongjun L (2012). Modeling and voltage control of variable-speed SCAG-based wind farm. Sci. Direct, Renewable Energy 42:28-35.

Hu J, Shang L, He Y, Zhu ZQ (2011). Direct Active and Reactive Power Regulation of Grid-Connected DC/AC Converters Using Sliding Mode Control Approach. IEEETrans. Power Electron. 26(1):210-222.

Pena R, Cardenas R, Blasco R, Asher G, Clare J (2001). A cage induction generator using back to back PWM converters for variable speed grid connected wind energy system. Proceeding in the 27th Conf. IEEE Ind. Electron. Soc. 2:1376-1381.

Shahab S, Fatemeh K, Tayebeh K, Zeynab K (2011). Maximum power point tracking of variable speed wind energy conversion system. Int. J. Phys. Sci. 6(30):6843-6851.

Tomonobu S, Yasutaka O, Yasuaki K, Motoki T, Atsushi Y, Naomitsu U, Toshihisa F (2009). Sensor-less maximum power point tracking control for wind generation system with squirrel cage induction generator. Sci. Direct, Renewable Energy 34(4):994-999.

Vivek A, Rakesh KA, Pravin P, Chetan P (2010). Novel Scheme for Rapid Tracking of Maximum Power Point in Wind Energy Generation Systems. IEEE Trans. Energy. Conv. 25(1):228-236.

Watthan S, Bunlung N (2011). An implementation of field oriented controlled SCIG for variable speed wind turbine. Proceding in 6th IEEE Conf. Ind. Electron. Appl. pp. 39-44.

Whei M, Chih M, Fsheng CH (2010). Fuzzy neural network output maximization control for sensorless wind energy conversion system. Sci. Direct, Energy 35(2):592-601.

Yulin Y, Yidong CH, Zhiyun J, Wang LI, Weiyang W (2010). Development of 22KW Experimental Platform for Wind Power Generation System Using SCIG. Proc. IEEE Int. Symp. Power Electron. Distrib. Gener. Syst. pp. 593-596.

Zhi D, Xu L, Williams BW (2009). Improved direct power control of grid-connected DC/AC converters. IEEE. Trans. Power Electron. 24(5): 1280-1292.

## Appendix

**Table 1.** Induction machine parameters.

| Parameter | Value |
|---|---|
| Rated power (kW) | 300 |
| Machine rated speed (tr/mn) | 1515 |
| Number of pole pairs | 2 |
| Stator resistance (mohms) | 6.3 |
| Rotor resistance (mohms) | 4.8 |
| Stator inductance (mH) | 11.8 |
| Rotor inductance (mH) | 11.6 |
| Magnetizing inductance (mH) | 11.6 |
| Rated frequency (Hz) | 50 |
| Nominal voltage (V) | 400 |

**Table 2.** Wind turbine parameters.

| Parameter | Value |
|---|---|
| Rated power (kW) | 300 |
| Optimal power coefficient | 0.475 |
| Optimal tip speed ratio | 8.1 |
| Turbine radius (m) | 14 |
| Nominal wind speed (m/s) | 12 |
| Minimum wind speed (m/s) | 4 |
| Gear box | 1:23 |
| Equivalent moment of inertia ($kg.m^2$) | 50 |
| Power control | Pitch control |

**Table 3.** Interconnecting grid parameters.

| Parameter | Value |
|---|---|
| Dc-bus voltage (V) | 760 |
| Dc-bus capacitor (mF) | 100 |
| Filter resistance (mohms) | 5 |
| Filter inductance (mH) | 0.5 |